

1 **SUPPLEMENT**

**Simultaneous tracers and a unified model of positional and mass isotopomers for
quantification of metabolic flux in liver**

2 **Stanislaw Deja**¹, Xiaorong Fu¹, Justin A. Fletcher¹, Blanka Kucejova¹, Jeffrey D. Browning², Jamey D.
3 Young^{3,*}, Shawn C. Burgess^{1,*}

4 ¹ Center for Human Nutrition, The University of Texas Southwestern Medical Center, Dallas, TX 75390, USA

5 ² Department of Clinical Nutrition, The University of Texas Southwestern Medical Center, Dallas, TX 75390, USA

6 ³ Department of Chemical and Biomolecular Engineering, Department of Molecular Physiology and Biophysics,
7 Vanderbilt University, Nashville, TN 37235, USA

8 **SUPPLEMENTARY RESULTS**

9

10 **Constraining body water ²H enrichment improves NMR but not GC-MS model-regressed**
11 **flux estimates**

12 The ²H enrichment of glucose is a function of precursor, or body water (enrichment of
13 ²H₂O). Thus, a measurement of ²H₂O body water enrichment can be used as an additional
14 constraint when fitting NMR or GC-MS isotopomer data to models of hepatic metabolism using
15 MFA. The ²H₂O enrichment in plasma was measured by ²H NMR using the natural ²H
16 abundance of acetone as a reference (**Figure S4A**) as previously reported (Jones et al.,
17 2001a), and could be quantify enrichments as low as 0.1% (**Figure S4B**). All plasma samples
18 were found to be close to 4% (**Figure S4D**), nearly identical to the targeted body water
19 enrichment based on ²H₂O injection. Though not measured, perfused livers must have a ²H₂O
20 enrichment of 3% based on volumes used to prepare the media (**Figure S4C**). In either case,
21 this information improved the regression of NMR data, but not GC-MS data. The discrepancy
22 may be related to the total lack of absolute enrichment information in the ²H NMR spectrum of
23 glucose, but precise information about absolute enrichment (e.g., M+0 versus M+1) in the mass
24 spectra of glucose fragments. When body water ²H enrichment was left as a free parameter that
25 could be adjusted during model-based regression of GC-MS data, the predicted body ²H₂O
26 enrichment was close to the assumed (**Figure S4C**) or measured (**Figure S4D**) values. Thus,
27 constraining the model to exact ²H enrichment adds information for fitting NMR data, but
28 apparently over-constrains GC-MS data.

29

30 **Testing the agreement of NMR and GC-MS flux estimates**

31 Every measurement implies some degree of error thus, when two independent methods
32 are used to measure the same variable, neither may provide an unequivocally correct answer.
33 Correlation analysis was used to assess the relationship between flux values obtained from
34 NMR and GC-MS measurements (main text and **Figure 7**). Passing-Bablok (PB) regression and
35 Bland Altman (BA) analysis were also used to estimate the degree of agreement between the
36 two methods of flux quantification.

37 **Passing-Bablok regression of flux estimates**

38 PB regression is a nonparametric method of fitting a straight line to a set of paired
39 variables (x and y). PB does not assume measurement error to be normally distributed and is
40 robust against outliers. To overcome the influence of outliers, the method estimates the slope
41 by calculating the median of all slopes that can be formed from all possible pairs; thus, it reports
42 slope and intercept values that can differ from the results obtained using standard least-squares
43 regression analysis (**Table S4**). We used PB regression to determine the existence and type of
44 differences between NMR and GC-MS based flux estimates by using following criteria:

- 45 1. Does the slope confidence interval (CI) enclose the value of 1? If no, there is
46 evidence for proportional differences between the analyzed methods.
- 47 2. Does the intercept CI enclose the value of 0? If no, there is evidence for constant
48 differences (bias) between the analyzed methods.
- 49 3. The PB procedure is valid only when flux values obtained using NMR and GC-
50 MS showed a linear relationship.

51 Indeed, PB regression indicated the presence of either constant or proportional bias in
52 all fluxes but V_{CS} , which had nearly identical values by both methods (**Table S4**). The $V_{Glycerol}$ flux
53 could not be analyzed since it did not meet the requirement of linearity (**Figure 7, Table S4**).
54 $V_{Glycogen}$ showed evidence for proportional differences, while V_{PEP} , V_{PEPCK} and V_{PK+ME} showed

55 both evidence for proportional and constant differences between methods (**Table S4**). These
56 results suggest that the variance of measurement error is not constant over the range of studied
57 flux values, and the variability increases with the magnitude of the flux estimates.

58 **Bland-Altman analysis of flux estimates**

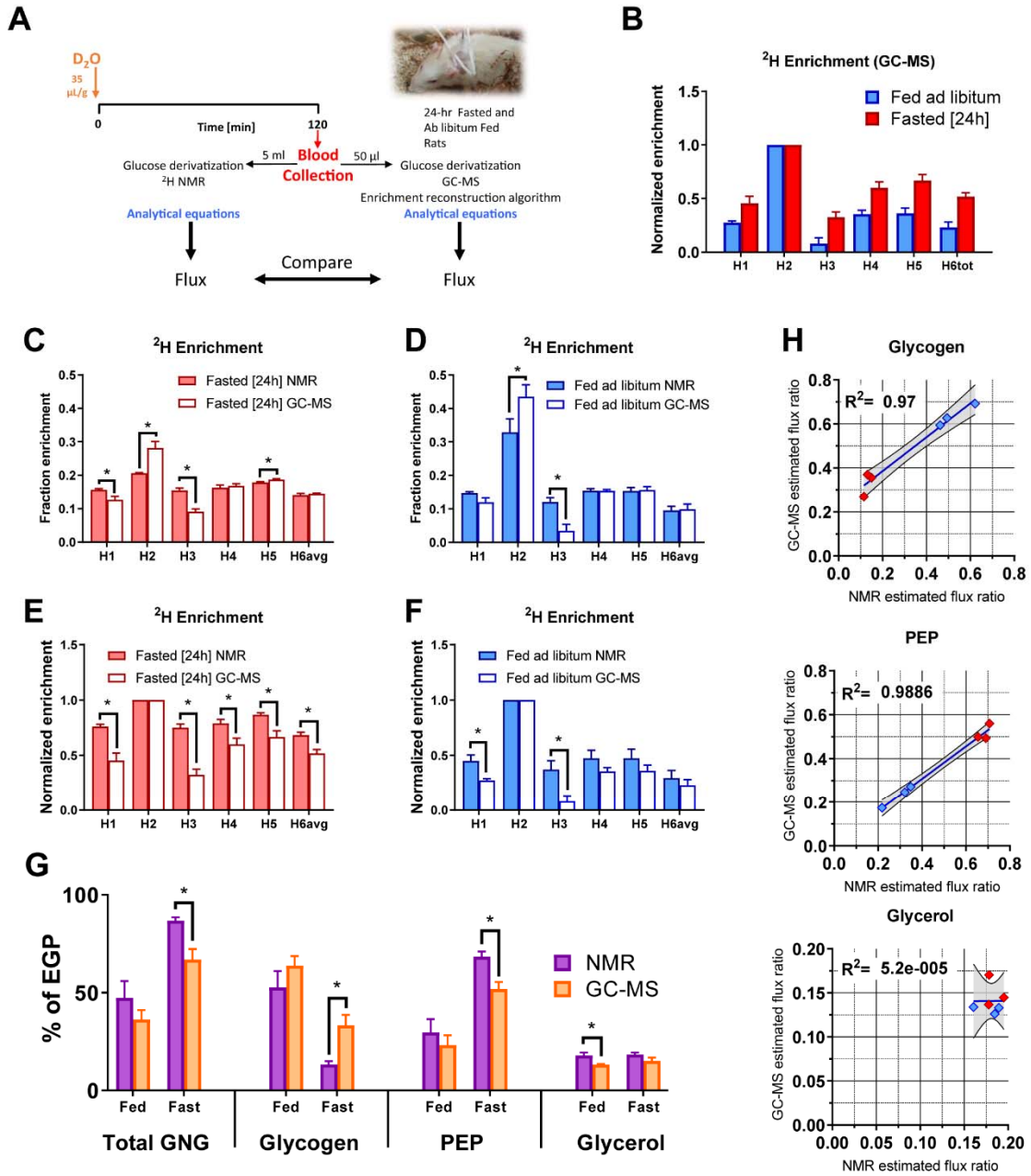
59 Unlike PB regression, which only examines the existence of differences, BA analysis
60 quantifies the magnitude of differences between the methods. In BA analysis, the difference or
61 the mean % difference of the two paired measurements is plotted against the mean of the two
62 measurements (**Figure S5**). BA analysis assumes the mean of the methods is correct and
63 reports bias and range of agreement within 95%, but does not determine if the agreement is
64 sufficient. Therefore, we used BA analysis to quantify bias for the fluxes that were flagged by PB
65 regression.

66 We found that V_{Glycogen} was negatively and proportionally different (-45.8%) between
67 NMR and GC-MS methods (**Figure S5**). Indeed, both methods detected glycogen depletion;
68 however, they differed when glycogen was a large contributor to EGP. The relatively large %
69 bias was partially driven by differences between glycogen-depleted samples (where small
70 absolute differences resulted in large % differences). Thus, either GC-MS overestimated, or
71 NMR underestimated glycogen contribution to EGP. However, the latter seems rather unlikely,
72 due to perfect distinction between positions H2 and H5 in the NMR spectrum of MAG.
73 Therefore, we concluded that GC-MS reports slightly higher glycogen contribution (as discussed
74 in the main text).

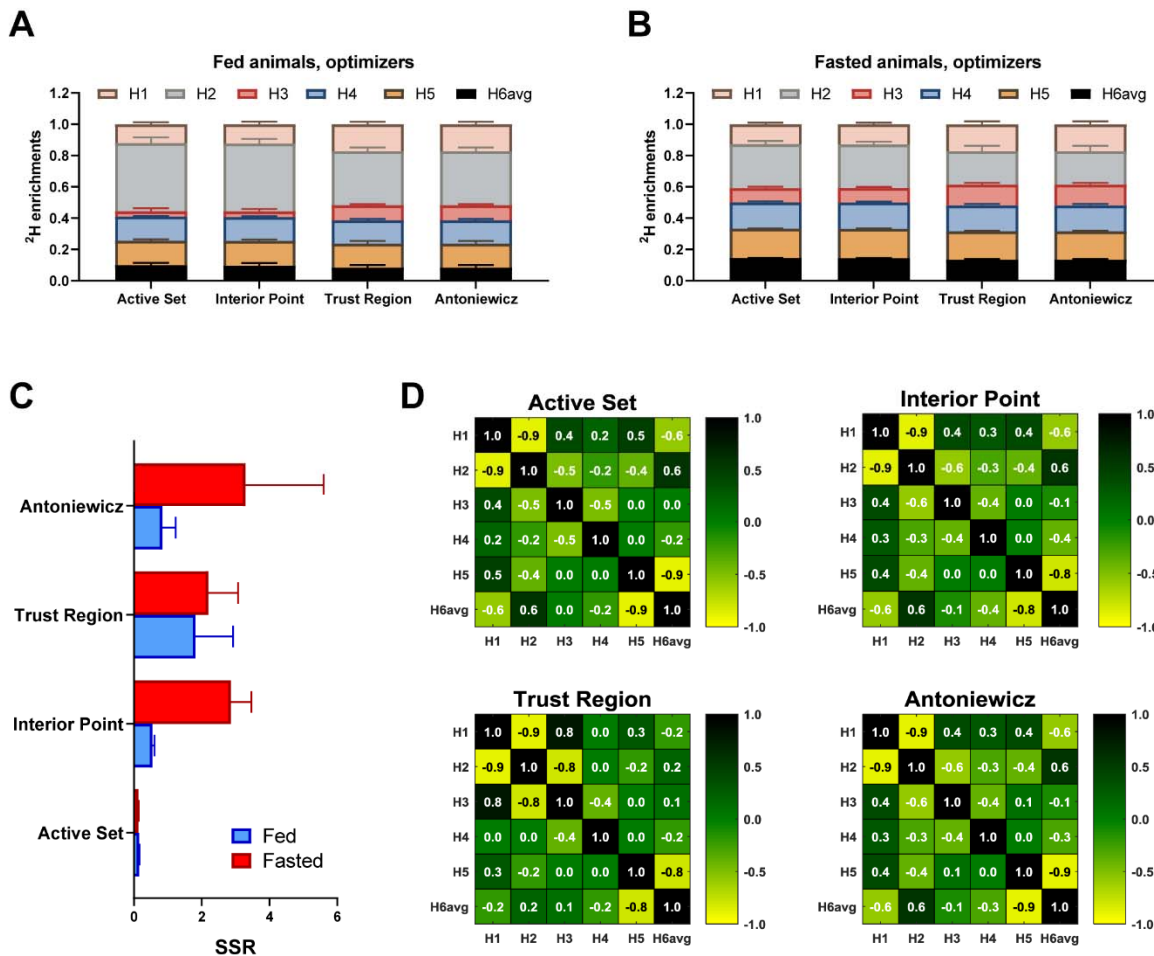
75 On the other hand, V_{PEP} (+9.4%), V_{PEPCK} (+16.7%) and $V_{\text{PK+ME}}$ (+24.1%) showed positive
76 constant and proportional differences for NMR compared to GC-MS (**Table S4**). Interestingly, all
77 three of these fluxes rely strongly on the presence of a distinct quartet isotopomer in the ^{13}C
78 NMR spectrum. However, GC-MS estimation of these fluxes requires deconvolution of many

79 overlapping mass isotopomers, which could lead to greater variability. The variation between
80 NMR and GC-MS in estimates of cataplerosis/anaplerosis may be related to differences in
81 estimates of ^{13}C M+3 isotopomers (i.e., [1,2,3- $^{13}\text{C}_3$]glucose and [4,5,6- $^{13}\text{C}_3$]glucose) or ^2H M+1
82 isotopomers. The latter is likely, inasmuch as GC-MS would estimate lower V_{PEP} due to a higher
83 estimation of V_{Glycogen} based on ^2H isotopomers. Such a shift in the contribution between
84 glycogen and PEP would also affect V_{PEPCK} and $V_{\text{PK+ME}}$ since all these fluxes are tightly
85 connected by stoichiometric relationships. Finally, V_{CS} showed no differences in PB regression;
86 thus, we consider the methods to agree on this flux, although BA quantified a slight (-13.6%)
87 difference between NMR and GC-MS.

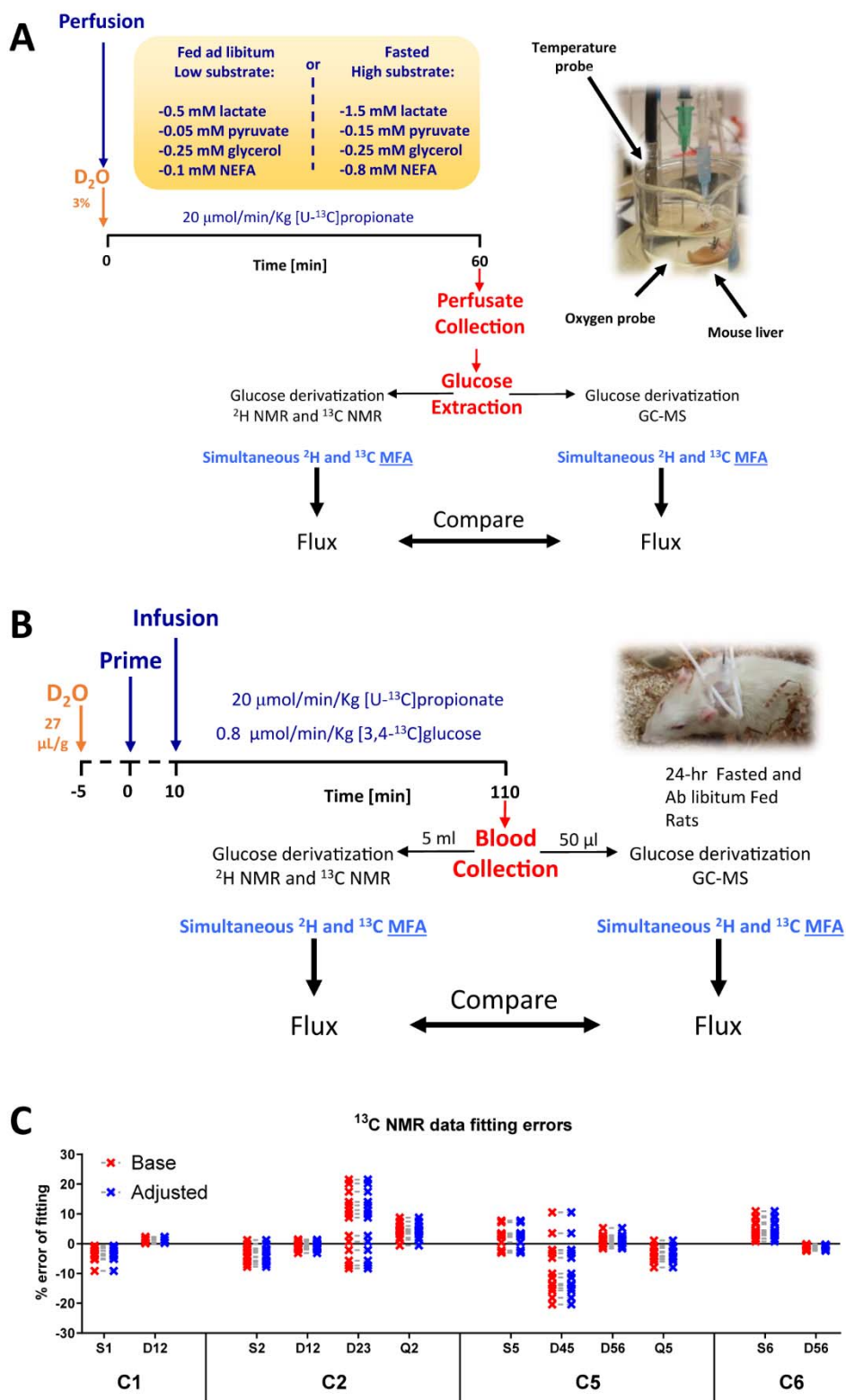
88 In conclusion, although both methods correlate well, they report different flux values.
89 These biases should be taken into account when comparing studies where fluxes were obtained
90 using NMR and GC-MS. However, when a single method is used, we expect that it will detect
91 changes in fluxes precisely.



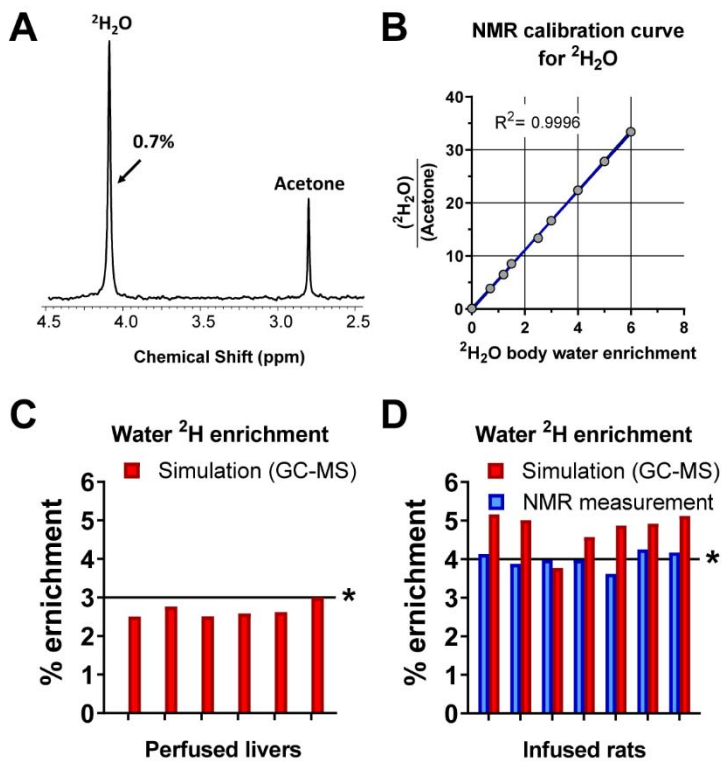
94 **Figure S1. Determination of glucose labeling from $^2\text{H}_2\text{O}$ by ^2H NMR and GC-MS. (A)**
95 Experimental setup of $^2\text{H}_2\text{O}$ glucose labeling *in vivo* in rats. After 120 min, blood was collected
96 and divided into aliquots for parallel analysis of positional ^2H enrichment followed by calculation
97 of metabolic fluxes using Landau's analytical equations (*Materials and Methods* Section 2.12),
98 **(B)** Fractional enrichment of glucose obtained from fed *ad libitum* and 24h-fasted rats analyzed
99 using GC-MS, **(C)** Fractional enrichment of glucose obtained from 24h fasted rats analyzed
100 using ^2H NMR and GC-MS. **(D)** Fractional enrichment of glucose obtained from fed *ad libitum*
101 rats analyzed using ^2H NMR and GC-MS. **(E)** Glucose labeling normalized to position H2
102 obtained from 24h fasted rats analyzed using ^2H NMR and GC-MS. **(F)** Glucose labeling
103 normalized to position H2 obtained from fed *ad libitum* rats analyzed using ^2H NMR and GC-MS.
104 **(G)** Differences in estimations of fluxes contributing to EGP between ^2H NMR and GC-MS. **(H)**
105 Correlation between gluconeogenic flux ratios calculated using ^2H NMR and predicted ^2H
106 labeling from GC-MS data. n=3 per group, *p < 0.05



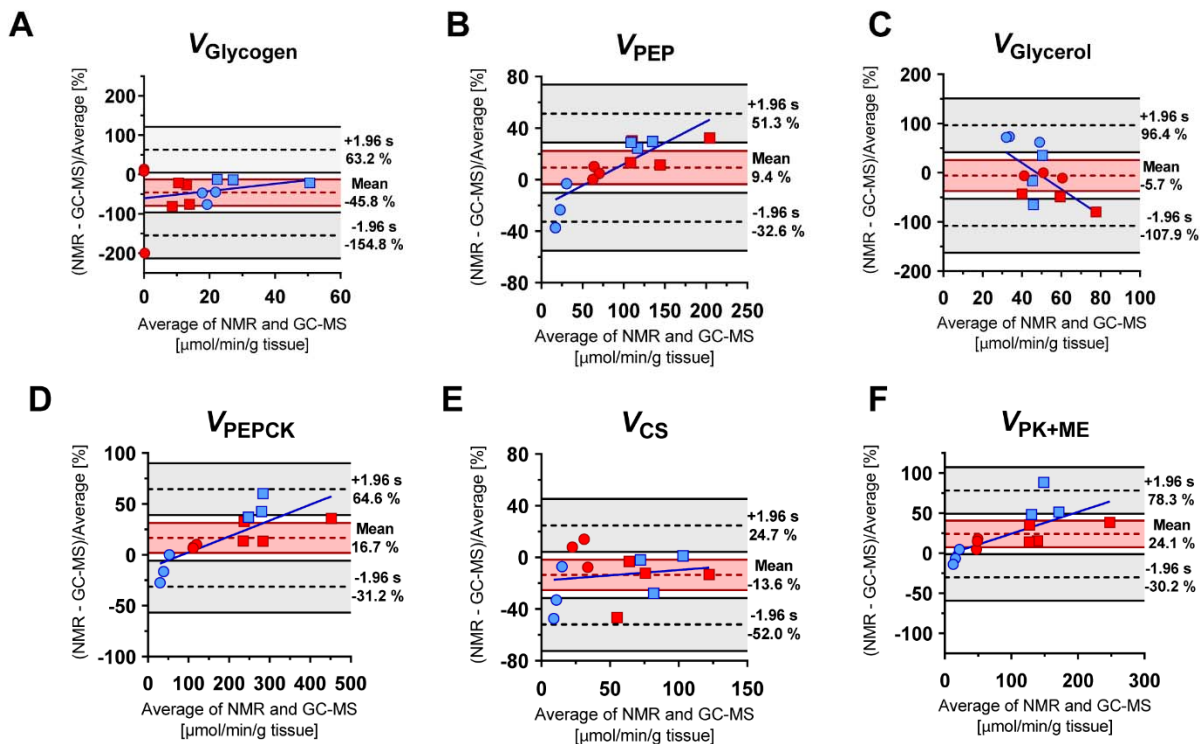
109 **Figure S2. Comparison of various optimizers used to estimate glucose ^2H enrichments**
110 **from least-squares regression of GC-MS data.** Three MATLAB quadratic programming
111 solvers (active set, interior point, and trust region) were compared to the custom solver used by
112 Antoniewicz et al. (2011). Unweighted least-squares regression was performed assuming 0.3
113 mol% error in the raw MID measurements. **(A)** Fractional ^2H enrichments of glucose obtained
114 from fed *ad libitum* rats, **(B)** Fractional ^2H enrichments of glucose obtained from 24h-fasted rats,
115 **(C)** Best-fit sum-of-squared residuals (SSRs) obtained from each solver, **(D)** Normalized
116 parameter covariance matrices of estimated enrichments averaged over all samples. Error bars
117 indicate SD (n=3).



120 **Figure S3. Double and triple tracer experiments.** (A) Experimental setup of double tracer
121 liver perfusion experiment (B) Experimental setup of triple tracer *in vivo* infusion in rats (C)
122 Percent errors of fitting ^{13}C NMR data to base and adjusted model.

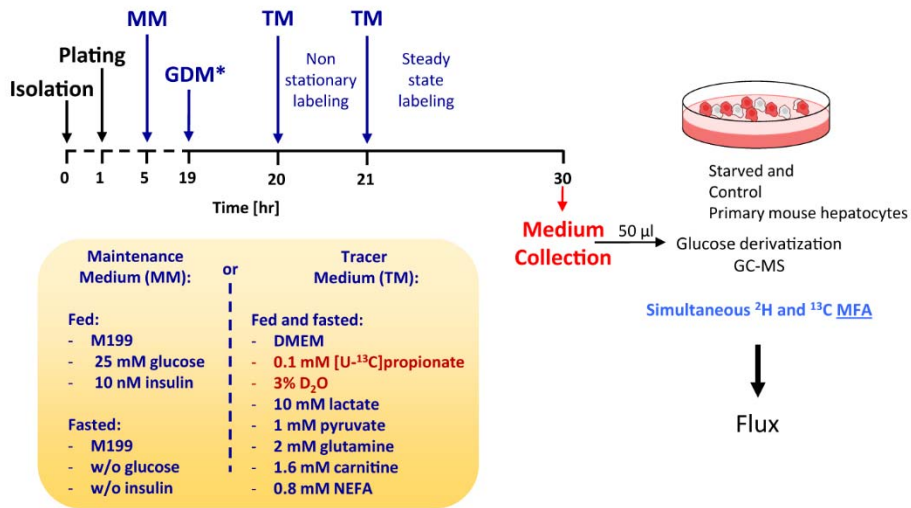


125 **Figure S4. Effect of body water enrichment.** (A) ^2H NMR spectrum used for quantification of
126 $^2\text{H}_2\text{O}$ enrichment in body water – note that acetone ^2H signal used as a reference originates
127 from the natural deuterium abundance, (B) calibration curve for relationship between $^2\text{H}_2\text{O}$
128 enrichment in body water and the ratio of NMR signals ($^2\text{H}_2\text{O}$)/(Acetone), (C,D) $^2\text{H}_2\text{O}$ enrichment
129 values based on simulation (from regression of GC-MS glucose data) and exact ^2H NMR
130 measurements in (C) perfused livers and (D) tracer infusions in rats. Expected water ^2H
131 enrichments are marked with horizontal line and asterisk (*).



134 **Figure S5. Bland-Altman analysis of agreement between NMR and GC-MS based flux**
135 **estimates.** Squares – tracer infusions in rats, circles – perfused mouse livers, blue – fed
136 condition, red – fasted condition. All fluxes are reported in $\mu\text{mol/g liver/hr}$. **(A)** V_{Glycogen} , **(B)** V_{PEP} ,
137 **(C)** V_{Glycerol} , **(D)** V_{PEPCK} , **(E)** V_{CS} , **(F)** $V_{\text{PK+ME}}$.

138 **Figure S6**



139

140 **Figure S6. Glucose labeling using double tracer method – *in vitro* primary mouse**
141 **hepatocytes.** Experimental setup of double tracer *in vitro* experiment. GDM – glycogen
142 depletion media was additionally used in fasted condition.

143 **Table S1. Metabolic network used for flux modeling.**

Flux	Reaction	Base model	Adjusted model
V _{Inf}	Gluc.inf (AaBbCcDdEeFfg) -> Gluc.ext (AaBbCcDdEeFfg)	+	+
V _{EGP}	H6P (AaBbCcDdEeFfg) -> Gluc.ext (AaBbCcDdEeFfg)	+	+
V _{Glycogen}	Glycogen (AaBbCcDdEeFfg) + H (h) -> H6P (AaBbCcDdEeFfg) + H (b)	+	+
V _{GNG}	T3P (CcBhAab) + T3P (DdEeFfg) + H (i) -> H6P (AbBiCcDdEeFfg) + H (h) + H (a)	+	+
V _{GAPDH}	BPG (ABbCcd) + H (e) + H (f) -> T3P (AeBfCcd) + H (b)	+	+
V _{Glycerol}	Glycerol (AaeBbCcd) + H (f) -> T3P (AeBfCcd) + H (a) + H (b)	+	+
V _{PEP}	PEP (ABCcd) + H (b) -> BPG (ABbCcd)	+	+
V _{PK+ME}	PEP (ABCab) + H (c) -> Pyr (ABCabc)	+	+
V _{LDH}	Lac (ABbCcde) -> Pyr (ABCcde) + H (b)	+	+
V _{PC}	Pyr (ABCcde) + CO ₂ (D) + H (f) + H (g) -> 0.5*Oac (ABCfgD) + 0.5*Oac (DCBfgA) + H (c) + H (d) + H (e)	+	+
V _{PEPCK}	Oac (ABCabD) -> PEP (ABCab) + CO ₂ (D)	+	+
V _{FAT}	FAT (BCabc) -> AcCoA (BCabc)	+	+
V _{CS}	Oac (ABCcdD) + AcCoA (EFfgh) -> Cit (DCcdBFfgEA) + H (h)	+	+
V _{IDH}	Cit (ABabCDcdEF) + H (e) -> Akg (ABCEaDcdE) + H (b) + CO ₂ (F)	+	+
V _{OGDH}	Akg (ABCabDcdE) -> SucCoA (BCabDcdE) + CO ₂ (A)	+	+
V _{PCC}	PropCoA (ABabCcde) + CO ₂ (D) -> SucCoA (ACcdBabD) + H (e)	+	+
V _{SDH}	SucCoA (ABabCcdD) + H (e) + H (f) -> 0.5*Oac (ABCefD) + 0.5*Oac (DCBefA) + H (a) + H (b) + H (c) + H (d)	+	+
V _{Hinf}	H.inf (a) -> H (a)	+	+
V _{Hsink}	H -> Sink	+	+
V* _{Glyc-Aldo}	Glycerol (AaeBbCcd) + H (f) + H (g) -> T3P (AgBfCcd) + H (a) + H (b) + H (e)	X	+
V* _{TPI-KIE}	H6P (AaBbCcDdEeFfg) + H.src (h) -> H6P (AaBbChDdEeFfg) + H (c)	X	+
V* _{PMI}	H6P (AaBbCcDdEeFfg) + H (h) -> H6P (AhBbCcDdEeFfg) + H (a)	X	+
V* _{TAL}	H6P (AaBbCcDdEeFfg) + T3P (HhJjKkm) + H (n) -> H6P (AaBbCcHhJjKkm) + T3P (DdEnFfg) + H (e)	X	X

144 Atom transitions are denoted by letters: capital for carbon atoms and lower case for protons.

145 Additional tested assumptions are labeled with an asterisk (*). Note that V_{Inf} was only used for

146 triple tracer experiments where [3,4-¹³C₂]glucose was infused *in vivo*. Green + denotes

147 reactions that were used in the model.

148 **Table S2. Accuracy and precision of MIDs measured from mouse blood**

149

Fragment (formula)			M+0	M+1	M+2	M+3	M+4
DIO	m/z 301 (C14H21O7)	exp	84.4 ± 0.03	13.2 ± 0.01	2.2 ± 0.01	0.2 ± 0.00	0.0 ± 0.01
		theory	84.2	13.4	2.2	0.2	0.0
MOX	m/z 145 (C6H11O3N)	exp	92.1 ± 0.07	6.7 ± 0.01	1.0 ± 0.02	0.1 ± 0.00	0.1 ± 0.00
		theory	92.5	6.7	0.8	0.0	0.0
ALDO	m/z 173 (C8H13O4)	exp	90.4 ± 0.02	8.0 ± 0.01	1.1 ± 0.01	0.1 ± 0.00	0.0 ± 0.00
		theory	90.6	8.3	1.1	0.1	0.0
	m/z 259 (C12H19O6)	exp	86.5 ± 0.01	11.5 ± 0.02	1.8 ± 0.02	0.2 ± 0.01	0.0 ± 0.01
		theory	86.2	11.8	1.8	0.2	0.0
	m/z 284 (C13H18O6N)	exp	84.8 ± 0.05	12.7 ± 0.05	2.0 ± 0.01	0.2 ± 0.02	0.1 ± 0.02
		theory	85.0	12.8	1.9	0.2	0.0
	m/z 370 (C17H24O8N)	exp	81.3 ± 0.09	15.5 ± 0.07	2.9 ± 0.01	0.4 ± 0.01	0.0 ± 0.01
		theory	80.9	15.9	2.8	0.4	0.0

150 Experimental (exp) and theoretical (theory) MID abundances of three investigated glucose
151 derivatives. Molar percent abundances (mol %) are reported as mean ± SD, n = 4. Maximum
152 deviation was 0.4% and measured precision was below 0.1%. Note that this result satisfies the
153 accuracy criteria (accuracy at least 0.5%, precision at least 0.1%) used for selection of these six
154 glucose m/z fragments in original work by Antoniewicz (2011).

155 **Table S3. Comparison of GC-MS based estimation of glucose ²H enrichment with exact**
 156 **NMR enrichments**

157

			Fed				Fasted				p value ^a
			Rat1	Rat2	Rat6	Mean ± SD	Rat3	Rat4	Rat5	Mean ± SD	
Glucose fractional ² H enrichment %	H1	NMR	15.0	14.3	14.9	14.7 ± 0.4	15.5	15.5	16.0	15.7 ± 0.3	0.03
		GC-MS	11.5	11.1	13.4	12.0 ± 1.2	12.7	11.7	13.7	12.7 ± 1.0	0.52
		p value ^b				0.05				0.03	
	H2	NMR	29.8	31.4	37.4	32.9 ± 4.0	20.7	20.6	20.4	20.6 ± 0.2	0.03
		GC-MS	40.4	42.9	47.4	43.5 ± 3.6	28.8	29.7	25.9	28.1 ± 2.0	0.01
		p value ^b				0.03				0.02	
	H3	NMR	12.8	12.9	10.5	12.1 ± 1.3	16.2	14.7	15.5	15.5 ± 0.7	0.03
GC-MS		5.3	3.7	1.4	3.5 ± 2.0	9.4	8.1	9.7	9.1 ± 0.8	0.02	
	p value ^b				0.00				0.00		
H4	NMR	16.0	15.5	14.9	15.4 ± 0.6	16.3	17.0	15.4	16.3 ± 0.8	0.23	
	GC-MS	15.5	15.7	15.0	15.4 ± 0.4	16.1	17.2	17.2	16.8 ± 0.6	0.04	
	p value ^b				0.90				0.41		
H5	NMR	16.0	15.9	14.2	15.4 ± 1.0	17.6	17.9	18.1	17.9 ± 0.2	0.05	
	GC-MS	16.4	16.0	14.6	15.7 ± 0.9	18.6	18.7	18.9	18.7 ± 0.2	0.03	
	p value ^b				0.74				0.01		
H6avg	NMR	10.4	10.1	8.1	9.5 ± 1.2	13.6	14.2	14.5	14.1 ± 0.4	0.01	
	GC-MS	11.0	10.6	8.2	9.9 ± 1.5	14.4	14.6	14.5	14.5 ± 0.1	0.03	
	p value ^b				0.74				0.23		
% EGP	Glycogen	NMR	46.2	49.4	62.2	52.6 ± 8.4	15.0	13.2	11.5	13.2 ± 1.7	0.01
		GC-MS	59.5	62.7	69.2	63.8 ± 5.0	35.6	37.0	26.9	33.2 ± 5.4	0.00
		p value ^b				0.14				0.02	
Glycerol	NMR	18.9	18.5	16.1	17.8 ± 1.5	19.5	17.8	17.8	18.4 ± 1.0	0.64	
	GC-MS	13.3	12.6	13.4	13.1 ± 0.4	14.5	13.7	17.0	15.1 ± 1.8	0.19	
	p value ^b				0.03				0.06		
PEP	NMR	34.9	32.1	21.8	29.6 ± 6.9	65.5	69.0	70.7	68.4 ± 2.6	0.01	
	GC-MS	27.2	24.7	17.4	23.1 ± 5.1	50.0	49.4	56.0	51.8 ± 3.7	0.00	
	p value ^b				0.27				0.00		

158 ^a Student's t test comparing fed and fasted conditions

159 ^b Student's t test comparing NMR and GC-MS data for individual positions

160

161 **Table S4. Analysis of agreement between methods**

Liner regression statistics		V _{Glycogen}	V _{PEP}	V _{PEPCK}	V _{PK+ME}	V _{CS}	V _{Glycerol}
Goodness of Fit	P value	<0.0001	<0.0001	<0.0001	<0.0001	<0.0001	0.7552
	r ²	0.9215	0.9741	0.9305	0.8649	0.945	0.009207
	r	0.9599	0.9870	0.9646	0.9300	0.9721	0.0960
	Slope	1.17	0.6842	0.6204	0.5691	1.08	-0.2332
	Intercept	3.421	14.3	28.55	13.85	2.259	63.76
Passing Bablok regression statistics							
Slope	Value	1.2329	0.6757	0.6358	0.6396	1.0725	N/A
	CI [LB]	1.0707	0.622	0.5274	0.4915	0.9327	N/A
	CI [UB]	1.9757	0.818	0.821	0.7799	1.2786	N/A
	Proportional differences? ^a	Yes	Yes	Yes	Yes	No	N/A
Intercept	Value	0.4006	11.8454	22.6028	9.0768	0.215	N/A
	CI [LB]	-4.9571	6.4599	10.2231	3.8916	-8.3192	N/A
	CI [UB]	2.5748	18.9534	47.1028	19.4755	5.8618	N/A
	Constant differences? ^b	No	Yes	Yes	Yes	No	N/A
Bland Altman bias analysis							
Bias [%]	Value	-45.8	9.4	16.7	24.1	-13.6	-5.7
	CI [LB]	-79.4	-3.6	1.9	7.3	-25.4	-37.2
	CI [UB]	-12.2	22.3	31.4	40.8	-1.8	25.7

162 CI – confidence interval, LB – lower boundary, UB – upper boundary

163 ^a Does the slope CI enclose the value of 1? If no, there is evidence for proportional difference
 164 between analyzed methods.

165 ^b Does the intercept CI enclose the value of 0? If no, there is evidence for constant differences
 166 (bias) between analyzed methods.